ACS Catalysis

pubs.acs.org/acscatalysis

Research Article

Manganese-Catalyzed Dehydrogenative Synthesis of Urea Derivatives and Polyureas

Aniekan Ekpenyong Owen, Annika Preiss,† Angus McLuskie,† Chang Gao,† Gavin Peters, Michael Bühl,* and Amit Kumar*

Cite This: *ACS Catal.* 2022, 12, 6923−6933

Read Online

ACCESS | Metrics & More | Article Recommendations | Supporting Information

ABSTRACT: Urea derivatives have significant applications in the synthesis of resin precursors, dyes, agrochemicals, and pharmaceutical drugs. Furthermore, polyureas are useful plastics with applications in coating, adhesive, and biomedical industries. However, the conventional methods for the synthesis of urea derivatives and polyureas involve toxic reagents such as (di)-isocyanates, phosgene, CO, and azides. We present here the synthesis of (poly)ureas using much less toxic reagents—(di)-amines and methanol—via a catalytic dehydrogenative coupling process. The reaction is catalyzed by a pincer complex of an earth-abundant metal, manganese, and liberates H_2 gas, valuable by itself, as the only byproduct, making the overall process highly atom-economic. A broad variety of symmetrical and unsymmetrical urea derivatives and polyureas have been synthesized in moderate to quantitative yields using this catalytic protocol. Mechanistic insights have also been provided using experiments and DFT computation, suggesting that the reaction proceeds via an isocyanate intermediate.

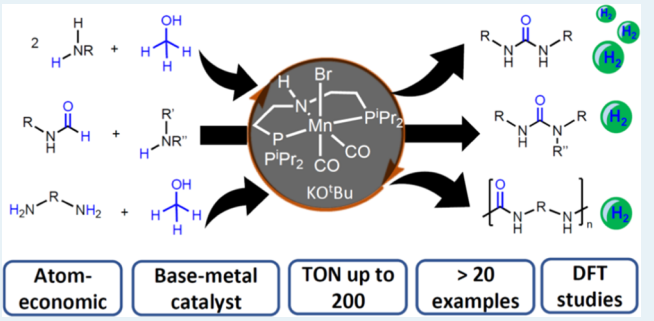

KEYWORDS: *catalysis, dehydrogenation, manganese, methanol, pincer, polyurea, urea*

INTRODUCTION

Urea derivatives are prevalent organic compounds with a variety of applications such as resin precursors,[1] dyes,[2] agrochemicals,[3,4] and pharmaceutical drugs[5,6] and in supramolecular chemistry.[7] Additionally, polyureas are useful classes of plastics with a range of applications for construction materials (e.g., coatings, adhesives)[8] and biomedical industry (e.g., drug delivery)[9] and have a current annual market of USD 885 million.[10] The current industrial methods for the synthesis of urea derivatives or polyureas involve the reaction of amines or diamines with highly toxic reagents such as phosgene,[11] (di)isocyanates,[12] or CO.[13] Reaction of CO_2 with (di)amines for the synthesis of (poly)ureas have also been reported, but they suffer from drawbacks such as the use of harsh reaction conditions (e.g., temperature > 150 °C, pressure > 40 bar) and limited substrate scope.[14−17] Thus, the development of an atom-economic, safer, and sustainable route for the synthesis of (poly)ureas will be highly valuable.

Reactions based on catalytic dehydrogenative coupling are green and atom-economic routes for the synthesis of organic compounds.[18,19] Several carbonyl compounds such as ketones, esters, and amides, along with polymers such as polyesters,[20] and polyamides,[21,22] can be synthesized using the approach of acceptorless catalytic dehydrogenative coupling of alcohols and amines.[23−26] This approach has also been utilized for the synthesis of urea derivatives via the dehydrogenative coupling of amines and methanol. The first example of the synthesis of urea derivatives from the dehydrogenative coupling of amines and methanol was reported by Hong using a ruthenium-Macho-BH pincer catalyst (**A**, Figure 1).[27] A TON of up to 190 was reported for the synthesis of symmetrical ureas; however, the synthesis of unsymmetrical ureas was achieved using a complex two-step method and higher catalytic loading (TON < 15). Additionally, a catalyst based on precious metal such as ruthenium is less desirable, as it is expensive, less abundant, and sometimes toxic, which could be a concern if the target compound is a pharmaceutical drug. Several catalysts based on earth-abundant metals have been reported for the (de)hydrogenative transformation in the recent past.[28−30] Bernskoetter has recently reported the dehydrogenative coupling of amines with methanol for the synthesis of symmetrical urea derivatives using an iron-Macho pincer catalyst (**B**, Figure 1).[31] Unsymmetrical ureas were synthesized by the reaction of formamides with amines, albeit with a limited substrate scope. These are the only two catalysts reported in the past for the synthesis of a broad scope of

Received: February 17, 2022
Revised: May 12, 2022

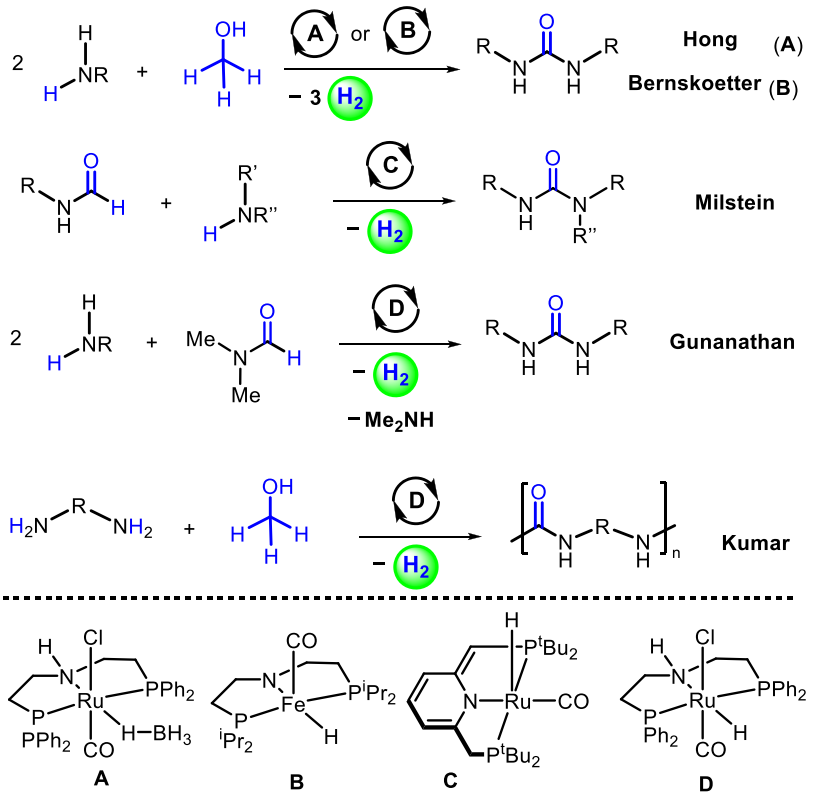

Figure 1. Previous reports on the dehydrogenative synthesis of (poly)ureas.

urea derivatives from the dehydrogenative coupling of amines and methanol. Prakash[32] and Milstein[33] have also independently studied the dehydrogenative coupling of methanol with diamines to form cyclic ureas for the purpose of developing new hydrogen storage materials using ruthenium pincer catalysts. Along a similar direction, Milstein has recently reported the synthesis of urea derivatives from the dehydrogenative coupling of formamides with amines in the presence of a ruthenium PNP catalyst (**C**, Figure 1), where the formamide was shown to act as an isocyanate surrogate.[34] Gunanathan has reported the synthesis of urea derivatives from the dehydrogenative coupling of *N*,*N*-dimethylformamide (DMF) and amines in the presence of a ruthenium-Macho complex (**D**).[35] The reaction occurs via the formyl C−H activation of DMF, leading to the elimination of NMe_2H and the formation of CO that subsequently reacts with an amine in the presence of the complex **D** to form a urea derivative. The concept of the dehydrogenative synthesis of ureas has been recently expanded by us for the synthesis of polyureas from the dehydrogenative coupling of diamines and methanol using the ruthenium-Macho complex **D** with a TON of up to 100 (Figure 1).[36] Along this line, recently, Robertson has reported the synthesis of high-molecular-weight polyureas from the dehydrogenative coupling of diformamides and diamines in the presence of the ruthenium pincer catalyst **A**.[37] Interestingly, the synthesis of urea derivatives was also demonstrated in one pot starting from ethyl formate and an amine that produced a formamide, which was subsequently reacted with an amine in the presence of the catalyst **A** to form a urea.

Replacement of the ruthenium-based catalyst with a catalyst of earth-abundant metal can make the overall process more cost-effective and sustainable. We present here the synthesis of a wide variety of urea derivatives and polyureas using a pincer complex of manganese, which is the third most abundant transition metal in the earth's crust.[38] This is the first example of a base metal catalyst for the dehydrogenative synthesis of polyureas and the second example for the dehydrogenative synthesis of urea derivatives after the recent report by Bernskoetter (Complex **B**, Figure 1).[31] Moreover, the use of methanol for the production of useful chemicals and materials makes the process beneficial to the circular economy as 100% renewable methanol can be directly produced from the hydrogenation of CO_2 or from biomass.[39]

We started our investigation by optimizing the catalytic conditions for the dehydrogenative coupling of octylamine with methanol in the presence of manganese complexes **1**−**6**, most of which have been reported for their excellent activity for (de)hydrogenative transformations.[40−44] Refluxing a toluene solution (120 °C, 24 h) of octylamine (1 mmol) and methanol (4 mmol) in the presence of the manganese-Macho pincer complex **1** (1 mol %) and KO^{t}Bu (4 mol %) under the open flow of nitrogen did not result in any conversion of octylamine presumably due to the low boiling point of methanol (64.7 °C at 1 bar). Interestingly, performing the same reaction in a sealed Young's flask resulted in the 50% conversion of octylamine. 1,3-dioctylurea was isolated in 44% yield (Table 1, entry 1). The PCy_2 analogue complex **2**, the P^tBu_2 analogue complex **3**, as well as the PPh_2 analogue complex **4** resulted in relatively lower yields of the 1,3-dioctylurea (entries 2−4), whereas no formation of the urea derivative was obtained in the case of complexes **5**−**6** under analogous conditions, as described in Table 1, entries 5−9. As complex **1** was found to be the most active precatalyst for this transformation, we used this complex for further optimization of reaction conditions. Using anisole as a solvent instead of toluene, keeping the remaining conditions the same resulted in a similar yield (45%, entry 10), whereas a

https://doi.org/10.1021/acscatal.2c00850
ACS Catal. 2022, 12, 6923−6933

Table 1. Optimization of Catalytic Conditions for the Dehydrogenative Coupling of Octylamine and Methanol[a]

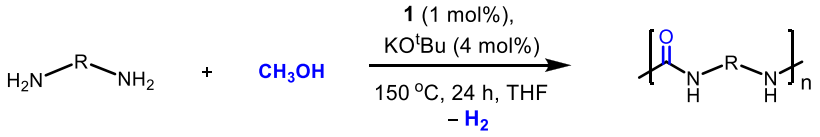

entry	complex	base	solvent	temperature (°C)	isolated yield (%)
1	**1** (1 mol %)	KO^{t}Bu (4 mol %)	toluene	120	44
2	**2** (1 mol %)	KO^{t}Bu (4 mol %)	toluene	120	38
3	**3** (1 mol %)	KO^{t}Bu (4 mol %)	toluene	120	25
4	**4** (1 mol %)	KO^{t}Bu (4 mol %)	toluene	120	10
5	**5** (1 mol %)	KO^{t}Bu (4 mol %)	toluene	120	0
6	**6a** (1 mol %)	KO^{t}Bu (4 mol %)	toluene	120	0
7	**6b** (1 mol %)	KO^{t}Bu (4 mol %)	toluene	120	0
8	**6a** (1 mol %)	KO^{t}Bu (4 mol %)	toluene	90	0
9	**6b** (1 mol %)	KO^{t}Bu (4 mol %)	toluene	90	0
10	**1** (1 mol %)	KO^{t}Bu (4 mol %)	anisole	120	45
11	**1** (1 mol %)	KO^{t}Bu (4 mol %)	THF	120	78
12	**1** (1 mol %)	KO^{t}Bu (4 mol %)	THF	150	98
13	**1** (1 mol %)	KOH (4 mol %)	THF	150	88
14	**1** (1 mol %)	K_2CO_3 (4 mol %)	THF	150	92
15	**1** (1 mol %)		THF	150	0
16	**1** (0.5 mol %)	KO^{t}Bu (2 mol %)	THF	150	97
17[b]	**1** (0.05 mol %)	KO^{t}Bu (0.2 mol %)	THF	150	68
18[c]	**1** (0.5 mol %)	KO^{t}Bu (2 mol %)	THF	150	45
19	**1** (0.5 mol %)	KO^{t}Bu (4 mol %)	neat	150	35
20		KO^{t}Bu (4 mol %)	THF	150	0
21	**1** (0.5 mol %)	KO^{t}Bu (0.5 mol %)	THF	150	41

[a]

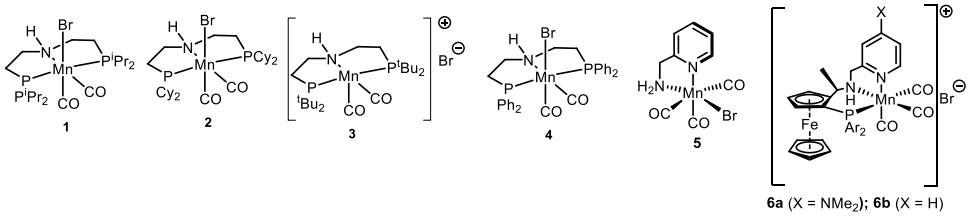

Catalytic conditions: octylamine (129 mg, 1 mmol), methanol (0.16 mL, 4 mmol), solvent (1 mL), 24 h. Ar = 3,5-Me_2-4-$OMeC_6H_2$ (reactions were carried out in a 100 mL Young's flask). [b]The reaction was carried in a 250 mL Young's flask using 3 mmol octylamine, 12 mmol methanol, and 3 mL THF for 24 h. [c]0.5 mmol of methanol was used.

significantly higher yield was obtained in the case of THF (78%, entry 11). Remarkably, when the temperature was increased to 150 °C while using THF as a solvent, a quantitative conversion of octylamine was obtained, and 1,3-dioctylurea was isolated in 98% yield by simple filtration and washing (with hexane) (entry 12). The use of other bases such as KOH and K_2CO_3 also showed excellent yields (entries 13 and 14), whereas no conversion of octylamine was obtained when the reaction was performed in the absence of a base (entry 15). Remarkably, reducing the catalytic loading to 0.5 mol % **1**; 2 mol % KO^{t}Bu also resulted in an almost quantitative yield of 1,3-dioctylurea, exhibiting a TON of 200 (entry 16). Further reduction of the catalytic loading to 0.05 mol % **1** and 0.2 mol % KO^{t}Bu resulted in 68% yield of 1,3-dioctylurea (entry 17). Interestingly, lowering the methanol amount to the reaction stoichiometric value, i.e., 0.5 mmol, resulted in a lower yield of 1,3-dioctylurea (entry 18), presumably due to the low boiling point (64.7 °C at 1 bar) of methanol keeping its significant part in the gas phase. A low yield (35%) was obtained when the reaction was performed under the neat condition without using any solvent (entry 19). Finally, performing a control experiment in the absence of a manganese catalyst but in the presence of 2 mol %, KO^{t}Bu did not result in any conversion of octylamine, suggestive of the crucial role of the manganese catalyst (entry 20). Interestingly, using 0.5 mol % of KO^{t}Bu in a combination of 0.5 mol % of complex **1** resulted in a lower yield of the product (41%), suggesting that an additional amount of the base, albeit in the catalytic amount, is needed for a higher yield (entry 21). The role of bases such as KO^{t}Bu in lowering the barrier of (de)hydrogenation reactions has been suggested before.[45,46] Interestingly, we do not observe the formation of imines or amines under our reaction conditions. This is related to a report by Beller, where the reaction of aromatic amines with methanol in the presence of complex **1** led to the formation of *N*-methylated amines.[47] However, 1 equivalent of KO^{t}Bu (relative to amine) was needed for the *N*-methylation reaction, and only aromatic amines such as aniline derivatives were reported in that case.[47] This is consistent with our results as we do not observe the formation of imines/amines using 2 mol % KO^{t}Bu (and complex **1**) and nonaromatic amines. Consistent with this observation, the computed driving force for dehydration of a model hemiaminal is much less favorable (slightly endergonic)

https://doi.org/10.1021/acscatal.2c00850
ACS Catal. 2022, 12, 6923−6933

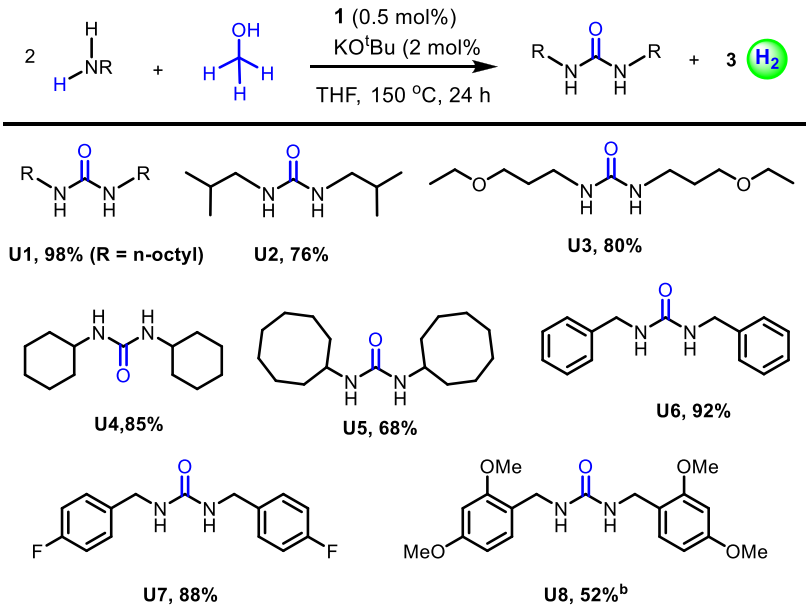

Figure 2. Dehydrogenative synthesis of symmetrical urea derivatives using the manganese complex **1**. **1** (0.005 mmol), KO^{t}Bu (0.02 mmol), amine (1 mmol), and methanol (0.16 mL, 4 mmol). ^{b}Yield estimated by ^{1}H NMR spectroscopy and GC-MS using 1,1′-diphenylethene as the internal standard. Reactions were carried out in 100 mL Young's flasks.

than that for dehydrogenation (vide infra, see Scheme S5 in the SI).

Upon optimization of catalytic conditions, we turned our attention to utilize this protocol to synthesize a variety of urea derivatives. Gratifyingly, using 0.5 mol % of complex **1** and 2 mol % KO^{t}Bu (THF, 150 °C, 24 h), a variety of symmetrical ureas were synthesized in moderate to excellent yields (Figure 2). As mentioned above, almost quantitative yield was obtained in the case of octylamine (**U1**). However, a slightly lower yield was obtained in the case of isobutyl amine, possibly due to the low boiling point of the amine (**U2**). Ethoxypropylamine also resulted in the corresponding urea in 80% yield (**U3**). Cyclohexyl amine afforded dicyclohexylurea in 85% yield (**U4**), whereas a relatively lower yield was obtained in the case of cyclooctyl amine (**U5**). Excellent yields were obtained in the case of benzylamine and 4-fluorobenzylamine (**U6**,**U7**). However, a poor yield was obtained in the case of 2,4-dimethoxybenzylamine (**U8**). Secondary amines such as *N*-methyl benzylamine, morpholine, and *N*,*N*-dicyclohexylamine did not result in any formation of the corresponding urea product even at a longer reaction time (72 h). Reluctance of the secondary amines toward the dehydrogenative synthesis of urea derivatives has been explained later using experiments and DFT computation (Schemes 1−3). Furthermore, catalytic reactions using aromatic amines such as aniline and 4-isopropylaniline were not successful, and the formation of only a trace amount (<5%) of the corresponding urea derivatives was observed.

Scheme 1. Possible Pathways for the Dehydrogenative Coupling of Formamide with an Amine to Form a Urea Derivative

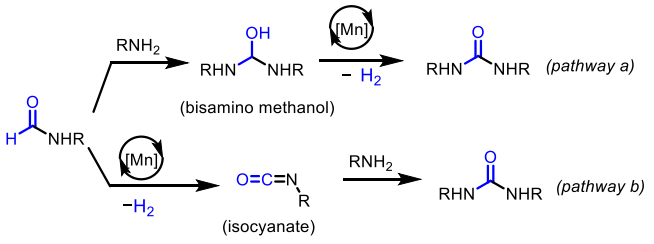

Although dehydrogenative synthesis of symmetrical urea derivatives using a manganese catalyst is interesting, several examples of urea-containing agrochemicals or pharmaceutical drugs involve unsymmetrical urea derivatives.[3−6] We utilized the approach of coupling formamide with amines to form unsymmetrical urea derivatives. This approach has been previously demonstrated by Milstein[34] and Bernskoetter[31] using a ruthenium and an iron pincer catalyst, respectively. Gratifyingly, using manganese pincer complex **1** (0.5 mol %) and KO^{t}Bu (2 mol %), several unsymmetrical urea derivatives were synthesized from the dehydrogenative coupling of formamides and amines, as described in Figure 3. Similar to the case of symmetrical urea derivatives, we were unable to synthesize unsymmetrical urea derivatives using aromatic amines and only a trace amount (<5% yield) of products was obtained from the reaction of formanilide with aromatic amines such as aniline and 4-isopropylaniline under the conditions described in Figure 3. In the case of the reaction of formanilide and 4-isopropylaniline, the transformylation product *N*-(4-isopropylphenyl)formamide was also observed. This could possibly be due to the poor nucleophilicity and better leaving group tendency of the aromatic amines in comparison to the aliphatic amines, as discussed below.

Consistent with this, DFT computation also showed that the thermodynamic driving forces for reaching the various intermediates along the reaction pathways (without involving the Mn catalyst) indeed become notably less favorable on going from methylamine to aniline (Section 17.4, SI).

Having accomplished the synthesis of a variety of urea derivatives, we expanded this catalytic protocol to demonstrate the dehydrogenative synthesis of polyureas which has not been achieved before using a catalyst of an earth-abundant metal. Gratifyingly, using 1 mol % of complex **1** and 4 mol % of KO^{t}Bu, we synthesized various polyureas from the dehydrogenative coupling of diamines and methanol in good to excellent yields

https://doi.org/10.1021/acscatal.2c00850
ACS Catal. 2022, 12, 6923−6933

Scheme 2. Control Experiments in Support of Pathway b

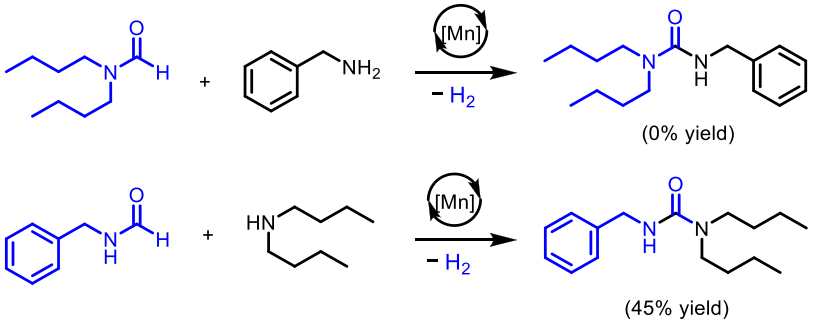

Scheme 3. Reaction of *N*-Methylformanilide with Octylamine and Benzylamine

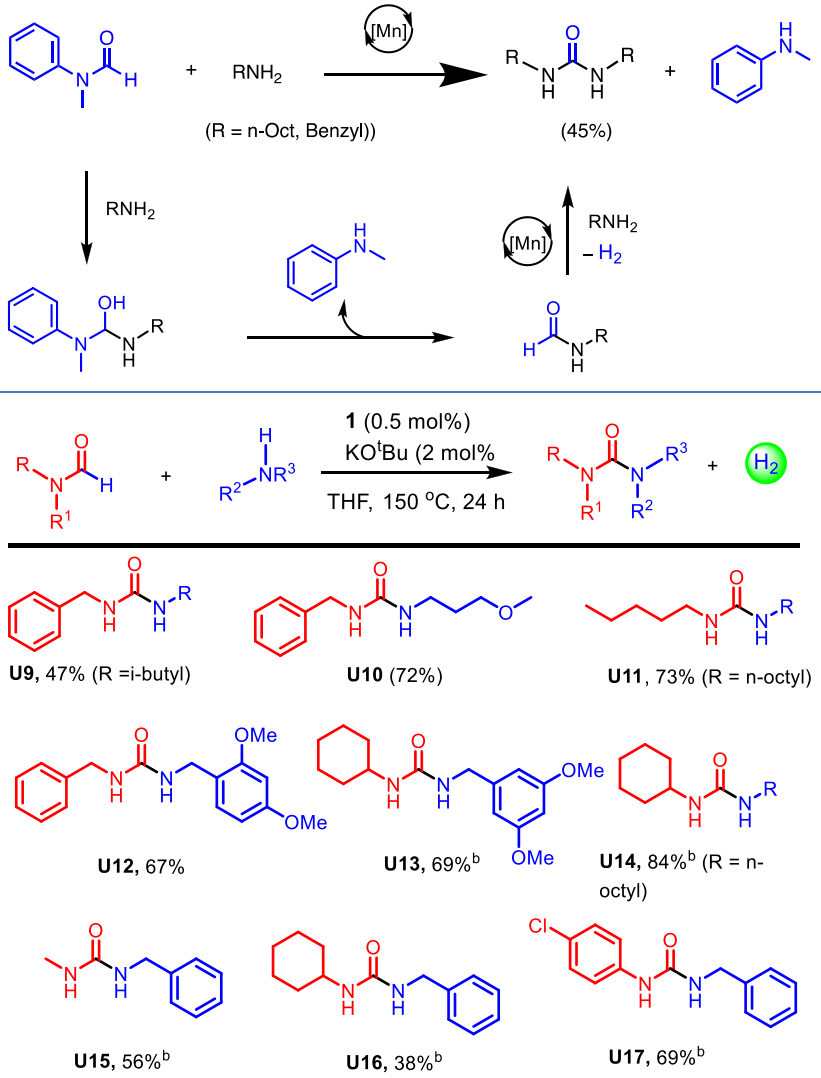

Figure 3. Dehydrogenative synthesis of unsymmetrical urea derivatives using the manganese complex **1**. **1** (0.005 mmol), KO^{t}Bu (0.02 mmol), formamide (1 mmol), and amine (1.5 mmol). ^{b}Yield estimated by ^{1}H NMR spectroscopy and GC-MS using 1,1′-diphenylethene as the internal standard. Reactions were carried out in 100 mL Young's flasks.

(Table 2). Interestingly, the dehydrogenative coupling of methanol with a renewable diamine Priamine 1074 (which is commercialized by the Croda, suggested structure shown in the SI) also resulted in the isolation of a solid polyurea in 80% yield (Table 2, entry 8). Considering that 100% renewable methanol is commercially available, this represents the formation of a polyurea, where each atom can be sourced from a renewable feedstock. Polyureas were characterized by NMR and IR spectroscopy as well as MALDI-TOF mass spectrometry. Due to the insolubility/poor solubility of polyureas in common organic solvents such as THF, water, and DMF, we were unable to estimate the molecular weight and PDI of polymers using GPC, and therefore the number average molecular weight (M_n) of the isolated polymers were estimated using ^{1}H NMR

https://doi.org/10.1021/acscatal.2c00850
ACS Catal. 2022, 12, 6923−6933

Table 2. Substrate Scope for the Dehydrogenative Synthesis of Polyureas.[a,b]

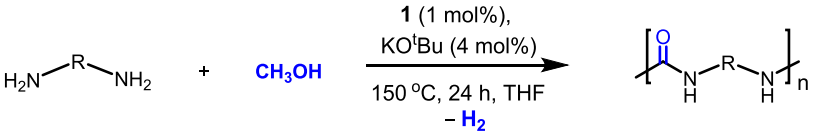

Entry	Diamine	Yield	M_n	T_d (°C)	T_c (°C)	T_g (°C)
1.	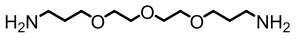	88%	9153	306	43	-30
2.	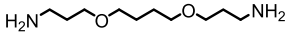	78%	15218	199	68	NA
3.	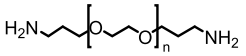	68%	6557	349	11	NA
4.	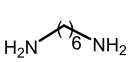	77%	3479	191	56	NA
5.	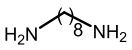	82%	2273	190	18, 78	NA
6.	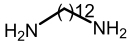	86%	3195	180	39, 93	45
7.[b]	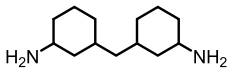	68%	1499	200	NA	NA
8.[b]	Priamine™ 1074	80%	-	348	NA	-25

[a]Catalytic conditions: Diamine (1 mmol), methanol (0.2 mL, 5 mmol), THF (1 mL), Complex **1** (0.01 mmol), and KO^{t}Bu (0.04 mmol). [b]Poor solubility observed in Trifluoroacetic acid. Reactions were carried out in 250 mL Young's flasks.

spectroscopy in *d*-TFA (trifluoroacetic acid) solvent through the end-group analysis, as previously reported by us.[36] The thermal stability of the polyureas was studied using the thermogravimetric analysis (TGA), which showed that the polyureas are stable up to 180−349 °C. Decomposition temperatures (T_d) were calculated by 5% weight loss in the TGA experiments. Crystallization temperature (T_c) and the glass transition temperature (T_g) were estimated by the DSC analysis and found to vary with the change of diamine. In comparison to the previously reported method using the ruthenium pincer catalyst **D** (Figure 1),[35] the estimated molecular weights (M_n) here are either similar, higher, or lower, depending on the choice of diamine. Aromatic diamines such as *p*-xylenediamine or *m*-xylenediamine were found to be unreactive and did not produce any polyurea, unlike the previous report using the ruthenium pincer catalyst **D** (Figure 1).[35] Another notable difference from the previously reported ruthenium[35] system is that the current manganese system is more selective toward the formation of urea, and other side reactions such as the aqueous reforming of methanol ($CH_3OH + H_2O \rightarrow CO_2 + 3H_2$) and decarbonylation are relatively less preferred. This conclusion is drawn based on the analysis of the evolved gas mixture using GC that showed much less concentration of CO_2 and CO (<0.5% combined yield, Figure S70) in comparison to that of the reported ruthenium system (6.5% combined yield).[35] H_2 gas was detected to be the major gas evolved from the reaction.

Having demonstrated the application of manganese pincer catalyst **1** for the dehydrogenative synthesis of a series of urea derivatives and polyureas, we carried out studies to gain insights into the mechanism of the dehydrogenative coupling reaction. When the catalytic reaction between octylamine and methanol as per the conditions of Table 1 entry 15 was stopped after 6 h, *N*-octylformamide and 1,3-dioctylurea (**U1**) were obtained in 10 and 30% yields, respectively. This suggests that the formation of urea derivatives occurs via a formamide intermediate presumably formed from the reaction of amine and methanol. This is in agreement with the ability of complex **1** to dehydrogenative couple formamides and amines to form urea derivatives, as demonstrated in Figure 3.

Based on the previous studies[27,31,34] and our mechanistic investigations, we suggest that the dehydrogenative synthesis of urea derivatives occurs via three steps, where each step releases one equivalent of H_2: (a) dehydrogenation of methanol to form formaldehyde, (b) dehydrogenative coupling of formaldehyde and amine to form a formamide, and (c) dehydrogenative coupling of formamide with another equivalent of amine to form a urea molecule. A few studies on the mechanistic investigations of the (de)hydrogenation reactions catalyzed by manganese complexes using DFT computation have been reported recently.[48−52] Along this line, we carried DFT calculations at the PBE0-D3/def2-TZVP/PCM//RI-BP86/def2-SVP/PCM level to get deeper insights into pathways for the synthesis of urea derivatives through the proposed three steps, as described below.

Step1: Dehydrogenation of Methanol to Formaldehyde. The manganese pincer complex **1** has been previously utilized for the dehydrogenative coupling of alcohols.[47,53−59] Based on the previous studies, we suggest that complex **1** reacts

https://doi.org/10.1021/acscatal.2c00850
ACS Catal. 2022, 12, 6923−6933

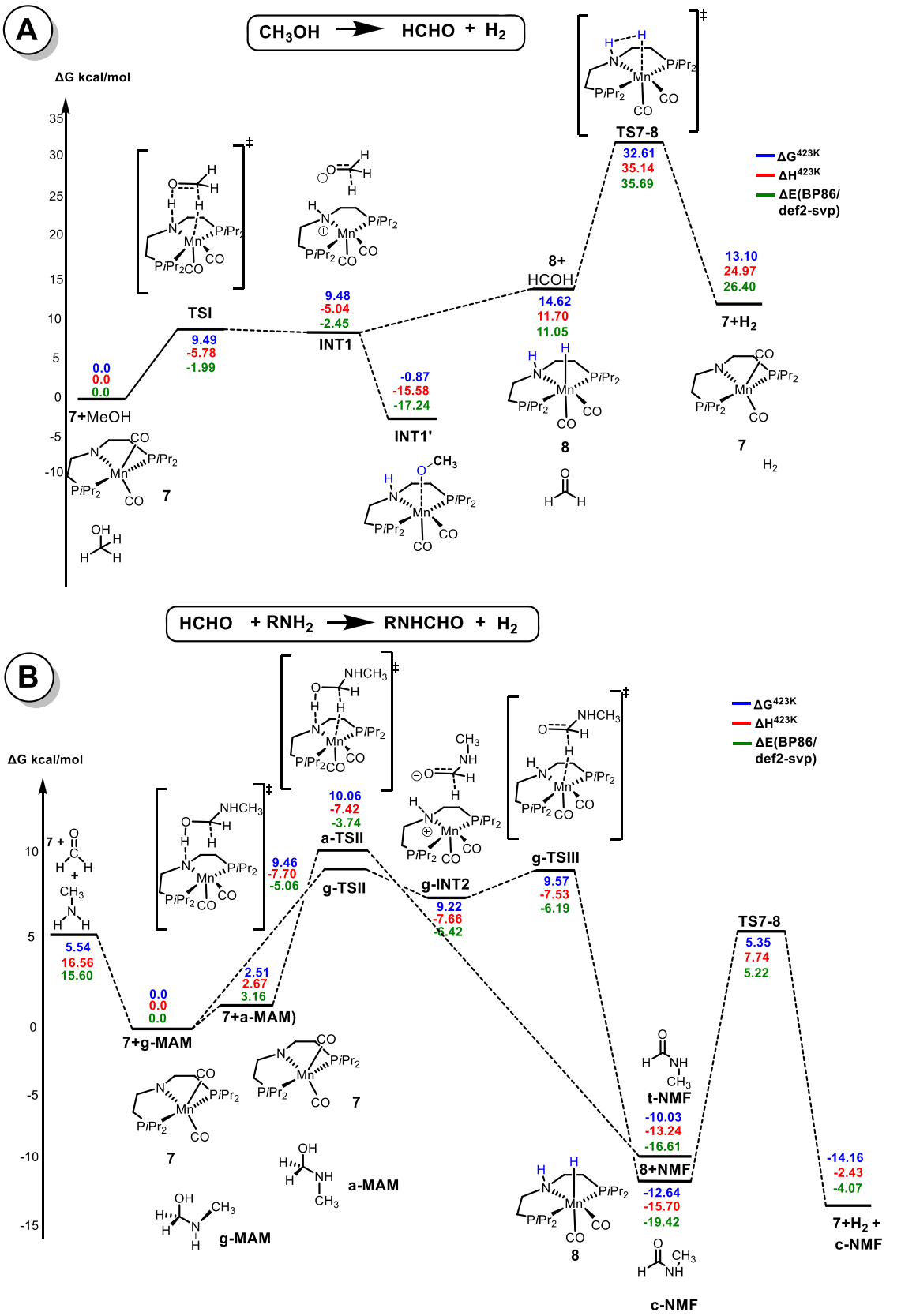

Figure 4. Free energy profile for (A) dehydrogenation of methanol using catalyst 7 to give formaldehyde and (B) synthesis of formamides from the dehydrogenative coupling of amines and methanol (using methylamine as a model substrate, PBE0-D3/def2-TZVP/PCM//RI-BP86/def2-SVP/PCM level).

with a base such as KO^{t}Bu to form the manganese−amido complex 7 that acts as an active species in catalysis. A pathway to the dehydrogenation of methanol to formaldehyde by complex 7 is outlined in Figure 4A. The amido site of the complex 7

https://doi.org/10.1021/acscatal.2c00850
ACS Catal. 2022, 12, 6923−6933

abstracts a proton from methanol through transition state **TSI** that appears to be shallow on the potential energy surface. A similar step has been reported for the DFT computation by Jiao and Beller for the dehydrogenation of methanol to formaldehyde.[60] **TSI** leads to the formation of a zwitterionic intermediate (**INT1**), with a driving force of ΔG = 9.48 kcal/mol. Formally, **INT1** can be described as a complex between a *N*-protonated complex (**7**-H$^+$) with methoxide ion (MeO$^-$), with a strong (agostic) interaction between a CH bond of the latter and the metal (BP86 optimized C···H and Mn···H distances of 1.18 and 1.86 Å, respectively). Starting from **INT1**, formaldehyde dissociates to form the Mn−hydride complex **8**, with no apparent barrier on the potential energy surface (in a scan at the BP86 level, the energy rises continuously as the C···H distance is increased).

The free energy for the full dissociation of formaldehyde is ΔG = 14.6 kcal/mol relative to the reactants (**7** + MeOH). The regeneration of the active catalyst can be achieved by the dehydrogenation of complex **8** proceeding through **TS7-8**. This is the rate-determining barrier with a free activation energy of $\Delta G^{\ddagger}$ = 32.6 kcal/mol relative to **7**. Involvement of protic substrates that can act as proton shuttles in that TS (such as methanol used as precursor, or traces of water) is indicated to reduce this barrier slightly (by 2.7−5.4 kcal/mol, see Scheme S6 in the SI). The overall process of the methanol dehydrogenation is computed to be endergonic by ΔG = 13.1 kcal/mol. It is noteworthy that the agostic intermediate **INT1** can rearrange to a zwitterionic methoxide complex **INT1′**, which is slightly lower in energy (by ΔG = −0.9 kcal/mol) than the reactant **7** + MeOH, but this does not affect the thermodynamics of the overall catalytic cycle, and the kinetics is affected only marginally. On the profile in Figure 4A, **INT1′** is an off-cycle intermediate that has to revert back to **INT1** for the reaction to proceed, raising the rate-determining barrier to $\Delta G^{\ddagger}$ = 33.9 kcal/mol between **TS7-8** and **INT1′**.

Step 2: Synthesis of Formamide from the Dehydrogenative Coupling of Formaldehyde and Amine. The formed formaldehyde reacts with an amine to form a hemiaminal that releases H_2 to form a formamide. Sola and Poater have recently reported a DFT study on the synthesis of formamides from the dehydrogenative coupling of methanol and amines catalyzed by a manganese pincer complex originally reported by Milstein.[61,62] The proposed mechanism suggests that formaldehyde and amine react off-metal to form a hemiaminal intermediate that subsequently gets dehydrogenated in the presence of the manganese pincer complex to form the formamide. Using methylamine as a model substrate, our DFT calculations align with this sequence. The proposed pathway for the dehydrogenative coupling of formaldehyde with the model methylamine to form *N*-methylformamide (NMF) and H_2 starts with the off-metal formation of a hemiaminal, *N*-methylaminomethanol (MAM). This intermediate can exist in two conformations, gauche and anti, with respect to the O−C−N−C dihedral angle. At our DFT level, the gauche conformer, **g-MAM**, is more stable than the anti-form (**a-MAM**) by 2.5 kcal/mol and its formation from the reactants is computed to be exergonic by ΔG = −5.5 kcal/mol. Likewise, the final product NMF can exist in two isomeric forms, *cis* and *trans*, relative to the (O)C−N(C) bond, of which *cis* (**c-NMF**) is more stable than *trans* by 2.6 kcal/mol. Dehydrogenation of the **MAM** conformer by the active catalyst **7** may be expected to proceed in analogy to that of MeOH (vide supra), with two possible pathways, one linking **g-MAM** with **c-NMF**, and the other linking the other isomers, i.e., anti-*N*-methylaminomethanol (**a-MAM**) with *trans*-*N*-methylformamide (**t-NMF**). The situation is slightly complicated by the observation that a stable agostic zwitterionic intermediate akin to **INT1** is only found on one of these pathways, namely starting from **g-MAM** (labeled **INT2**) via **g-TSII**. The analoguous TS on the anti pathway, **a-TSII**, does not connect to a zwitterionic intermediate but is a concerted TS for transfer of both H atoms (though asynchronous because protonation of the N atom of catalyst **7** occurs before hydride transfer to the metal), affording the product **t-NMF** directly. The rate-limiting step is again indicated to be the regeneration of the active catalyst **7** from **8** but now with an overall barrier $\Delta G^{\ddagger}$ of only 18.0 kcal/mol (13.6 kcal/mol with assistance by MeOH in the latter step). The production of formamide is thus indicated to be very rapid under the reaction conditions.

Step 3: Dehydrogenative Coupling of Formamide with Another Equivalent of Amine. The third step, that is, the dehydrogenative coupling of formamide and amine to form urea, can occur via two pathways (Scheme 1): (a) formamide can react with an amine to form a bisamino methanol (aminal)-type intermediate, followed by its subsequent dehydrogenation to form urea or (b) formamide can dehydrogenate to form an isocyanate that subsequently reacts with an amine to form urea. The mechanistic studies conducted by Milstein using the ruthenium pincer complex **C** suggested the latter pathway.[34]

We performed control experiments to verify which pathway is more likely to occur in the case of manganese. Our attempt to perform dehydrogenative coupling of a secondary amine such as morpholine or dicyclohexylamine with methanol to form substituted urea was not successful. Moreover, the reaction of benzylamine with *N*,*N*-dibutylformamide did not result in the formation of a urea derivative (Scheme 2). These are suggestive of the isocyanate pathway as an isocyanate intermediate will not be formed in the case of disubstituted formamide due to the lack of an N-H proton. Interestingly, a reaction of benzylformamide and *N*,*N*-dibutylamine resulted in the formation of the corresponding urea product in 45% yield as estimated by ^{1}H NMR spectroscopy (Scheme 2). It is noteworthy that both the above-mentioned reactions will form the same aminal intermediate as per the pathway a of Scheme 2. This experiment, thus, is supportive of the pathway b. However, lack of reactivity of *N*,*N*-dibutylformamide could also arise due to high steric bulk at the amide site.

To probe further into the role of steric bulk, we performed the reactions of *N*-methylformanilide with primary amines such as octylamine and benzylamine (Scheme 3). Although *N*-methylformanilide is a disubstituted formamide without N-H proton, it is less bulky compared to the *N*,*N*-dibutylformamide. Interestingly, in these cases, symmetrical urea derivatives (dioctylurea, dibenzylurea) were formed with *N*-methylaniline as the byproduct (observed by the GC-MS). We suggest these proceed via the reaction of *N*-methylformanilide with an amine to form an aminal intermediate, which instead of dehydrogenating eliminates *N*-methylaniline to form an *N*-alkyl formamide containing an N-H proton. The formamide reacts with the remaining amine to form the corresponding symmetrical urea derivative (Scheme 3). These experiments further support the hypothesis that the presence of an N-H proton on the formamide is crucial to the formation of urea derivatives.

Our DFT results fully agree with this interpretation. Dehydrogenation of formamide is predicted to proceed via a zwitterionic intermediate akin to that involved in methanol dehydrogenation (labeled **TSI** in Figure 4A), namely **INT3** in

https://doi.org/10.1021/acscatal.2c00850
ACS Catal. 2022, 12, 6923−6933

Figure 5, and a transition state (**TSV**) with a moderately high barrier of $\Delta G^{\ddagger}$ = 23.3 kcal/mol (Figure 5). As in the Mn-

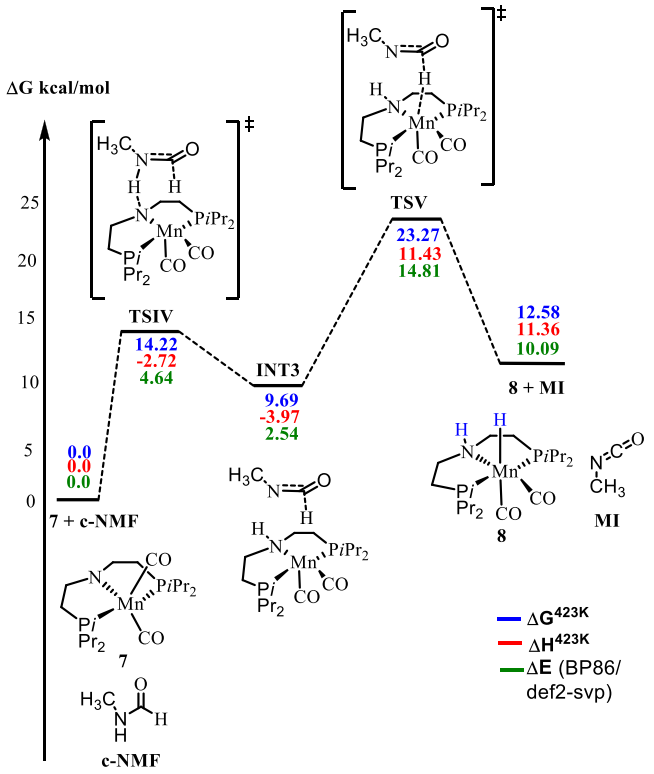

Figure 5. Key steps for isocyanate formation with the active catalyst **7** from DFT (using *cis-N*-methylformamide, **c-NMF**, and methyl isocyanide, **MI**, as model substrates, PBE0-D3/def2-TZVP/PCM//RI-BP86/def2-SVP/PCM level).

catalyzed dehydrogenation steps discussed above, regeneration of the active catalyst **7** from **8** is indicated to be rate-limiting with an overall barrier of $\Delta G^{\ddagger}$ = 30.6 kcal/mol (see full profile in Scheme S2). This barrier is similar to (and even slightly lower than) that for methanol dehydrogenation (32.6 kcal/mol, vide supra, Figure 4A), confirming the isocyanate pathway as a viable route (assistance by MeOH is computed to reduce both barriers by the same amount, 5.4 kcal/mol). The isocyanate product would be removed from this mixture through rapid reaction with an amine, affording the urea product (computed driving force for the model reaction $MeNCO + MeNH_2 \rightarrow N,N'$-dimethylurea is $\Delta G = -3.5$ kcal/mol at our DFT level). A similar methodology where formamides get dehydrogenated to isocyanates followed by their subsequent coupling with alcohols to form carbamates has also been recently reported by Bernskoetter and Hazari using an analogous iron pincer complex.[63]

In contrast, much higher barriers are computed for the aminal route (pathway a of Scheme 2). While catalytic dehydrogenation of a model aminal is indicated to be kinetically feasible at our DFT level, the formation of such an aminal from the formamide and alkylamine is so unfavorable (computed ΔG = 20.6 kcal/mol for the methylated models) that the overall barrier is raised to $\Delta G^{\ddagger}$ = 38.3 kcal/mol (see Schemes S4 and S5 in the SI). This value is significantly higher than that computed for the isocyanate route ($\Delta G^{\ddagger}$ = 30.6 kcal/mol, see above—again, MeOH assistance is computed to reduce both overall barriers by the same amount, 5.4 kcal/mol), suggesting that it is the latter pathway that is followed essentially exclusively, in full accord with the experiment.

CONCLUSIONS

In conclusion, we report here the dehydrogenative synthesis of urea derivatives and polyureas using a manganese pincer catalyst. Urea derivatives and polyureas are synthesized by the dehydrogenative coupling of (di)amines and methanol or using formamides and amines. Only one example of the earth-abundant metal catalyst (iron-Macho catalyst) has been reported in the past for the dehydrogenative synthesis of urea derivatives. Furthermore, this is the first example of an earth-abundant metal catalyst for the synthesis of polyureas from diamines and methanol. We also report here our mechanistic studies supported by both experiments and DFT computation and suggest that the formation of urea derivatives proceeds via an isocyanate intermediate. Overall, this methodology presents a sustainable alternative to the current state of the art for the production of ureas and polyureas by virtue of (a) being atom-economic, (b) using an earth-abundant metal catalyst, and (c) replacing toxic reagents such as phosgene and isocyanates with a renewable chemical—methanol.

ASSOCIATED CONTENT

Supporting Information

The Supporting Information is available free of charge at https://pubs.acs.org/doi/10.1021/acscatal.2c00850.

Synthesis and characterization details as well as the DFT computation (PDF)

AUTHOR INFORMATION

Corresponding Authors

Michael Bühl − *School of Chemistry, University of St. Andrews, St. Andrews KY169ST, U.K.*; Email: buehl@st-andrews.ac.uk

Amit Kumar − *School of Chemistry, University of St. Andrews, St. Andrews KY169ST, U.K.*; orcid.org/0000-0002-8175-8221; Email: ak336@st-andrews.ac.uk

Authors

Aniekan Ekpenyong Owen − *School of Chemistry, University of St. Andrews, St. Andrews KY169ST, U.K.*

Annika Preiss − *School of Chemistry, University of St. Andrews, St. Andrews KY169ST, U.K.*

Angus McLuskie − *School of Chemistry, University of St. Andrews, St. Andrews KY169ST, U.K.*

Chang Gao − *School of Chemistry, University of St. Andrews, St. Andrews KY169ST, U.K.*

Gavin Peters − *School of Chemistry, University of St. Andrews, St. Andrews KY169ST, U.K.*

Complete contact information is available at: https://pubs.acs.org/10.1021/acscatal.2c00850

Author Contributions

†A.P., A.M., and C.G. contributed equally.

Notes

The authors declare no competing financial interest.

The research data supporting this publication can be accessed at https://doi.org/10.17630/a924bc5f-7d77-4372-b0c3-69d02ef1d090.

https://doi.org/10.1021/acscatal.2c00850
ACS Catal. 2022, 12, 6923−6933

■ ACKNOWLEDGMENTS

A.K. thanks the Leverhulme Trust for an early career fellowship (ECF-2019-161). We thank Professor Matt Clarke and his research group (School of Chemistry, University of St. Andrews) for assisting with lab equipment/facilities and donating complexes **4** (by Nina Jeffrey) and **5**−**6** (by Conor Oates). M.B. wishes to thank the School of Chemistry and EaStCHEM for their support. A.E.O. gratefully acknowledges a fellowship from the Akwa Ibom State University (TETFund). Calculations were performed on a local compute cluster maintained by Dr. H. Früchtl. A.P. thanks the Royal Society of Chemistry for an undergraduate research bursary award. A.M. thanks the AD links foundation postgraduate research scholarship. The authors thank the Croda Europe Ltd. for their generous donation of Priamine diamines. The authors also thank Dr. Robert Tooze and Mr. Brian Boardman from the Drochaid Research Services Ltd. for their help with the GC.

■ REFERENCES

(1) Kumar, R. N.; Pizzi, A. Urea-Formaldehyde Resins. In *Adhesives for Wood and Lignocellulosic Materials*; Wiley, 2019; pp 61−100.
(2) Patel, M. J.; Tandel, R. C. Synthesis of Reactive Dyes by the Introduction of Phenyl Urea Derivatives into the Triazine Ring and Their Application on Different Fibers. *Mater. Today Proc.* **2021**, *46*, 6459−6464.
(3) Melnikov, N. N. *Derivatives of Urea and Thiourea BT - Chemistry of Pesticides*; Melnikov, N. N.; Gunther, F. A.; Gunther, J. D., Eds.; Springer US: New York, NY, 1971; pp 225−239.
(4) Morais, S. *Urea Pesticides*; Correia, M., Ed.; IntechOpen: Rijeka, Chapter 10, 2011.
(5) Ronchetti, R.; Moroni, G.; Carotti, A.; Gioiello, A.; Camaioni, E. Recent Advances in Urea- and Thiourea-Containing Compounds: Focus on Innovative Approaches in Medicinal Chemistry and Organic Synthesis. *RSC Med. Chem.* **2021**, *12*, 1046−1064.
(6) Ghosh, A. K.; Brindisi, M. Urea Derivatives in Modern Drug Discovery and Medicinal Chemistry. *J. Med. Chem.* **2020**, *63*, 2751−2788.
(7) Yokoya, M.; Kimura, S.; Yamanaka, M. Urea Derivatives as Functional Molecules: Supramolecular Capsules, Supramolecular Polymers, Supramolecular Gels, Artificial Hosts, and Catalysts. *Chem. - Eur. J.* **2021**, *27*, 5601−5614.
(8) Shojaei, B.; Najafi, M.; Yazdanbakhsh, A.; Abtahi, M.; Zhang, C. A Review on the Applications of Polyurea in the Construction Industry. *Polym. Adv. Technol.* **2021**, *32*, 2797−2812.
(9) Rocas, P.; Cusco, C.; Rocas, J.; Albericio, F. On the Importance of Polyurethane and Polyurea Nanosystems for Future Drug Delivery. *Curr. Drug Deliv.* **2018**, *15*, 37−43.
(10) PolyureaCoatings Market Global Forecast to 2025 | MarketsandMarkets. https://www.marketsandmarkets.com/Market-Reports/polyurea-coatings-market-152676861.html?gclid=Cj0KCQjw8rT8BRCbARIsALWiOvRwzrAtBwMcCRV3eXvOYKIdHfFk5OpjWw5rp5oVMIpe50yRVEX5LHcaAkN0EALw_wcB (accessed May 24, 2022).
(11) Bigi, F.; Maggi, R.; Sartori, G. Selected Syntheses of Ureas through Phosgene Substitutes. *Green Chem.* **2000**, *2*, 140−148.
(12) Mane, M.; Balaskar, R.; Gavade, S.; Pabrekar, P.; Mane, D. An Efficient and Greener Protocol towards Synthesis of Unsymmetrical N,N′-Biphenyl Urea. *Arab. J. Chem.* **2013**, *6*, 423−427.
(13) Guan, Z.-H.; Lei, H.; Chen, M.; Ren, Z.-H.; Bai, Y.; Wang, Y.-Y. Palladium-Catalyzed Carbonylation of Amines: Switchable Approaches to Carbamates and N,N′-Disubstituted Ureas. *Adv. Synth. Catal.* **2012**, *354*, 489−496.
(14) Wang, P.; Fei, Y.; Long, Y.; Deng, Y. Catalytic Polymerization of CO2 to Polyureas over K3PO4 Catalyst. *J. CO2 Util.* **2018**, *28*, 403−407.
(15) Wu, C.; Wang, J.; Chang, P.; Cheng, H.; Yu, Y.; Wu, Z.; Dong, D.; Zhao, F. Polyureas from Diamines and Carbon Dioxide: Synthesis, Structures and Properties. *Phys. Chem. Chem. Phys.* **2012**, *14*, 464−468.
(16) Jiang, S.; Cheng, H. Y.; Shi, R. H.; Wu, P. X.; Lin, W. W.; Zhang, C.; Arai, M.; Zhao, F. Y. Direct Synthesis of Polyurea Thermoplastics from CO2 and Diamines. *ACS Appl. Mater. Interfaces* **2019**, *11*, 47413−47421.
(17) Ying, Z.; Zhao, L.; Zhang, C.; Yu, Y.; Liu, T.; Cheng, H.; Zhao, F. Utilization of Carbon Dioxide to Build a Basic Block for Polymeric Materials: An Isocyanate-Free Route to Synthesize a Soluble Oligourea. *RSC Adv.* **2015**, *5*, 42095−42100.
(18) Kumar, A.; Gao, C. Homogeneous (De)Hydrogenative Catalysis for Circular Chemistry − Using Waste as a Resource. *ChemCatChem* **2021**, *13*, 1105−1134.
(19) Shimbayashi, T.; Fujita, K. I. Recent Advances in Homogeneous Catalysis via Metal−Ligand Cooperation Involving Aromatization and Dearomatization. *Catalysts* **2020**, *10*, No. 635.
(20) Hunsicker, D. M.; Dauphinais, B. C.; Mc Ilrath, S. P.; Robertson, N. J. Synthesis of High Molecular Weight Polyesters via In Vacuo Dehydrogenation Polymerization of Diols. *Macromol. Rapid Commun.* **2012**, *33*, 232−236.
(21) Gnanaprakasam, B.; Balaraman, E.; Gunanathan, C.; Milstein, D. Synthesis of Polyamides from Diols and Diamines with Liberation of H2. *J. Polym. Sci. Part A: Polym. Chem.* **2012**, *50*, 1755−1765.
(22) Zeng, H.; Guan, Z. Direct Synthesis of Polyamides via Catalytic Dehydrogenation of Diols and Diamines. *J. Am. Chem. Soc.* **2011**, *133*, 1159−1161.
(23) Gunanathan, C.; Milstein, D. Applications of Acceptorless Dehydrogenation and Related Transformations in Chemical Synthesis. *Science* **2013**, *341*, No. 6143.
(24) Crabtree, R. H. Homogeneous Transition Metal Catalysis of Acceptorless Dehydrogenative Alcohol Oxidation: Applications in Hydrogen Storage and to Heterocycle Synthesis. *Chem. Rev.* **2017**, *117*, 9228−9246.
(25) Bonitatibus, P. J.; Chakraborty, S.; Doherty, M. D.; Siclovan, O.; Jones, W. D.; Soloveichik, G. L. Reversible Catalytic Dehydrogenation of Alcohols for Energy Storage. *Proc. Natl. Acad. Sci. U.S.A* **2015**, *112*, 1687−1692.
(26) Heravi, M. R. P.; Hosseinian, A.; Rahmani, Z.; Ebadi, A.; Vessally, E. Transition-Metal-Catalyzed Dehydrogenative Coupling of Alcohols and Amines: A Novel and Atom-Economical Access to Amides. *J. Chin. Chem. Soc.* **2021**, *68*, 723−737.
(27) Kim, S. H.; Hong, S. H. Ruthenium-Catalyzed Urea Synthesis Using Methanol as the C1 Source. *Org. Lett.* **2016**, *18*, 212−215.
(28) Alig, L.; Fritz, M.; Schneider, S. First-Row Transition Metal (De)Hydrogenation Catalysis Based on Functional Pincer Ligands. *Chem. Rev.* **2019**, *119*, 2681−2751.
(29) Mukherjee, A.; Milstein, D. Homogeneous Catalysis by Cobalt and Manganese Pincer Complexes. *ACS Catal.* **2018**, *8*, 11435−11469.
(30) Piccirilli, L.; Lobo Justo Pinheiro, D.; Nielsen, M. Recent Progress with Pincer Transition Metal Catalysts for Sustainability. *Catalysts* **2020**, *10*, No. 773.
(31) Lane, E. M.; Hazari, N.; Bernskoetter, W. H. Iron-Catalyzed Urea Synthesis: Dehydrogenative Coupling of Methanol and Amines. *Chem. Sci.* **2018**, *9*, 4003−4008.
(32) Kothandaraman, J.; Kar, S.; Sen, R.; Goeppert, A.; Olah, G. A.; Prakash, G. K. S. Efficient Reversible Hydrogen Carrier System Based on Amine Reforming of Methanol. *J. Am. Chem. Soc.* **2017**, *139*, 2549−2552.
(33) Xie, Y.; Hu, P.; Ben-David, Y.; Milstein, D. A Reversible Liquid Organic Hydrogen Carrier System Based on Methanol-Ethylenediamine and Ethylene Urea. *Angew. Chem., Int. Ed.* **2019**, *58*, 5105−5109.
(34) Bruffaerts, J.; Von Wolff, N.; Diskin-Posner, Y.; Ben-David, Y.; Milstein, D. Formamides as Isocyanate Surrogates: A Mechanistically Driven Approach to the Development of Atom-Efficient, Selective Catalytic Syntheses of Ureas, Carbamates, and Heterocycles. *J. Am. Chem. Soc.* **2019**, *141*, 16486−16493.

https://doi.org/10.1021/acscatal.2c00850
ACS Catal. 2022, 12, 6923−6933

(35) Krishnakumar, V.; Chatterjee, B.; Gunanathan, C. Ruthenium-Catalyzed Urea Synthesis by N-H Activation of Amines. *Inorg. Chem.* **2017**, *56*, 7278−7284.
(36) Kumar, A.; Armstrong, D.; Peters, G.; Nagala, M.; Shirran, S. Direct Synthesis of Polyureas from the Dehydrogenative Coupling of Diamines and Methanol. *Chem. Commun.* **2021**, *57*, 6153−6156.
(37) Langsted, C. R.; Paulson, S. W.; Bomann, B. H.; Suhail, S.; Aguirre, J. A.; Saumer, E. J.; Baclasky, A. R.; Salmon, K. H.; Law, A. C.; Farmer, R. J.; Furchtenicht, C. J.; Stankowski, D. S.; Johnson, M. L.; Corcoran, L. G.; Dolan, C. C.; Carney, M. J.; Robertson, N. J. Isocyanate-Free Synthesis of Ureas and Polyureas via Ruthenium Catalyzed Dehydrogenation of Amines and Formamides. *J. Appl. Polym. Sci.* **2022**, *139*, No. 52088.
(38) Haynes, W. M. *The CRC Handbook of Chemistry and Physics*, 95th ed.; CRC Press: Fr. Boca Raton, 2015.
(39) Roode-Gutzmer, Q. I.; Kaiser, D.; Bertau, M. Renewable Methanol Synthesis. *ChemBioEng Rev.* **2019**, *6*, 209−236.
(40) Wang, Y.; Wang, M.; Li, Y.; Liu, Q. Homogeneous Manganese-Catalyzed Hydrogenation and Dehydrogenation Reactions. *Chem* **2021**, *7*, 1180−1223.
(41) Bruneau-Voisine, A.; Wang, D.; Dorcet, V.; Roisnel, T.; Darcel, C.; Sortais, J.-B. Transfer Hydrogenation of Carbonyl Derivatives Catalyzed by an Inexpensive Phosphine-Free Manganese Precatalyst. *Org. Lett.* **2017**, *19*, 3656−3659.
(42) Widegren, M. B.; Harkness, G. J.; Slawin, A. M. Z.; Cordes, D. B.; Clarke, M. L. A Highly Active Manganese Catalyst for Enantioselective Ketone and Ester Hydrogenation. *Angew. Chem., Int. Ed.* **2017**, *56*, 5825−5828.
(43) Oates, C. L.; Widegren, M. B.; Clarke, M. L. Manganese-Catalysed Transfer Hydrogenation of Esters. *Chem. Commun.* **2020**, *56*, 8635−8638.
(44) Zubar, V.; Haedler, A. T.; Schütte, M.; Hashmi, A. S. K.; Schaub, T. Hydrogenative Depolymerization of Polyurethanes Catalyzed by a Manganese Pincer Complex. *ChemSusChem* **2022**, *15*, No. e202101606.
(45) Alberico, E.; Lennox, A. J. J.; Vogt, L. K.; Jiao, H.; Baumann, W.; Drexler, H. J.; Nielsen, M.; Spannenberg, A.; Checinski, M. P.; Junge, H.; Beller, M. Unravelling the Mechanism of Basic Aqueous Methanol Dehydrogenation Catalyzed by Ru-PNP Pincer Complexes. *J. Am. Chem. Soc.* **2016**, *138*, 14890−14904.
(46) Nguyen, D. H.; Trivelli, X.; Capet, F.; Swesi, Y.; Favre-Réguillon, A.; Vanoye, L.; Dumeignil, F.; Gauvin, R. M. Deeper Mechanistic Insight into Ru Pincer-Mediated Acceptorless Dehydrogenative Coupling of Alcohols: Exchanges, Intermediates, and Deactivation Species. *ACS Catal.* **2018**, *8*, 4719−4734.
(47) Elangovan, S.; Neumann, J.; Sortais, J.-B.; Junge, K.; Darcel, C.; Beller, M. Efficient and Selective N-Alkylation of Amines with Alcohols Catalysed by Manganese Pincer Complexes. *Nat. Commun.* **2016**, *7*, No. 12641.
(48) Luque-Urrutia, J. A.; Solà, M.; Milstein, D.; Poater, A. Mechanism of the Manganese-Pincer-Catalyzed Acceptorless Dehydrogenative Coupling of Nitriles and Alcohols. *J. Am. Chem. Soc.* **2019**, *141*, 2398−2403.
(49) Masdemont, J.; Luque-Urrutia, J. A.; Gimferrer, M.; Milstein, D.; Poater, A. Mechanism of Coupling of Alcohols and Amines To Generate Aldimines and H2 by a Pincer Manganese Catalyst. *ACS Catal.* **2019**, *9*, 1662−1669.
(50) Borghs, J. C.; Azofra, L. M.; Biberger, T.; Linnenberg, O.; Cavallo, L.; Rueping, M.; El-Sepelgy, O. Manganese-Catalyzed Multicomponent Synthesis of Pyrroles through Acceptorless Dehydrogenation Hydrogen Autotransfer Catalysis: Experiment and Computation. *ChemSusChem* **2019**, *12*, 3083−3088.
(51) Azofra, L. M.; Poater, A. Diastereoselective Diazenyl Formation: The Key for Manganese-Catalysed Alcohol Conversion into (E)-Alkenes. *Dalton Trans.* **2019**, *48*, 14122−14127.
(52) Weber, S.; Glavic, M.; Stöger, B.; Pittenauer, E.; Podewitz, M.; Veiros, L. F.; Kirchner, K. Manganese-Catalyzed Dehydrogenative Silylation of Alkenes Following Two Parallel Inner-Sphere Pathways. *J. Am. Chem. Soc.* **2021**, *143*, 17825−17832.
(53) Peña-López, M.; Piehl, P.; Elangovan, S.; Neumann, H.; Beller, M. Manganese-Catalyzed Hydrogen-Autotransfer C−C Bond Formation: α-Alkylation of Ketones with Primary Alcohols. *Angew. Chem., Int. Ed.* **2016**, *55*, 14967−14971.
(54) Nguyen, D. H.; Trivelli, X.; Capet, F.; Paul, J.-F.; Dumeignil, F.; Gauvin, R. M. Manganese Pincer Complexes for the Base-Free, Acceptorless Dehydrogenative Coupling of Alcohols to Esters: Development, Scope, and Understanding. *ACS Catal.* **2017**, *7*, 2022−2032.
(55) Kaithal, A.; van Bonn, P.; Hölscher, M.; Leitner, W. Manganese(I)-Catalyzed β-Methylation of Alcohols Using Methanol as C1 Source. *Angew. Chem., Int. Ed.* **2020**, *59*, 215−220.
(56) Andérez-Fernández, M.; Vogt, L. K.; Fischer, S.; Zhou, W.; Jiao, H.; Garbe, M.; Elangovan, S.; Junge, K.; Junge, H.; Ludwig, R.; Beller, M. A Stable Manganese Pincer Catalyst for the Selective Dehydrogenation of Methanol. *Angew. Chem., Int. Ed.* **2017**, *56*, 559−562.
(57) Liu, Y.; Shao, Z.; Wang, Y.; Xu, L.; Yu, Z.; Liu, Q. Manganese-Catalyzed Selective Upgrading of Ethanol with Methanol into Isobutanol. *ChemSusChem* **2019**, *12*, 3069−3072.
(58) Fu, S.; Shao, Z.; Wang, Y.; Liu, Q. Manganese-Catalyzed Upgrading of Ethanol into 1-Butanol. *J. Am. Chem. Soc.* **2017**, *139*, 11941−11948.
(59) Tondreau, A. M.; Boncella, J. M. 1,2-Addition of Formic or Oxalic Acid to −N{CH2CH2(PiPr2)}2-Supported Mn(I) Dicarbonyl Complexes and the Manganese-Mediated Decomposition of Formic Acid. *Organometallics* **2016**, *35*, 2049−2052.
(60) Wei, Z.; de Aguirre, A.; Junge, K.; Beller, M.; Jiao, H. Exploring the Mechanisms of Aqueous Methanol Dehydrogenation Catalyzed by Defined PNP Mn and Re Pincer Complexes under Base-Free as Well as Strong Base Conditions. *Catal. Sci. Technol.* **2018**, *8*, 3649−3665.
(61) Luque-Urrutia, J. A.; Pèlachs, T.; Solà, M.; Poater, A. Double-Carrousel Mechanism for Mn-Catalyzed Dehydrogenative Amide Synthesis from Alcohols and Amines. *ACS Catal.* **2021**, *11*, 6155−6161.
(62) Kumar, A.; Espinosa-Jalapa, N. A.; Leitus, G.; Diskin-Posner, Y.; Avram, L.; Milstein, D. Direct Synthesis of Amides by Dehydrogenative Coupling of Amines with Either Alcohols or Esters: Manganese Pincer Complex as Catalyst. *Angew. Chem., Int. Ed.* **2017**, *56*, 14992−14996.
(63) Townsend, T. M.; Bernskoetter, W. H.; Hazari, N.; Mercado, B. Q. Dehydrogenative Synthesis of Carbamates from Formamides and Alcohols using a Pincer-Supported Iron Catalyst. *ACS Catal.* **2021**, *11*, 10614−10624.

https://doi.org/10.1021/acscatal.2c00850
ACS Catal. 2022, 12, 6923−6933